Available online at www.sciencedirect.com
SCIENCE DIRECT®
International Journal of Multiphase Flow 31 (2005) 25–51
International Journal of Multiphase Flow
www.elsevier.com/locate/ijmulflow

Venturi-assisted liquid removal from the sump of a gas well

J.D. Sherwood *, D.I.H. Atkinson

Schlumberger Cambridge Research, High Cross, Madingley Road, Cambridge CB3 0EL, UK

Received 15 February 2004; received in revised form 24 August 2004

Abstract

Gas wells produce not only gas, but also a small amount of liquid which, being dense, can collect at the bottom of the well. The well may slowly fill with liquid, and gas production is reduced, or stopped completely, when the perforations through which gas flows into the well are submerged. A simple Venturi pump can be used to re-disperse the liquid into the gas flowing to the surface. The pressure available for lifting liquid into the Venturi throat is not large, and it is therefore advantageous if gas is mixed into the liquid, thereby reducing the effective density of the mixture which has to be lifted. An analysis based solely on Bernoulli's equation and hydrostatic pressures is surprisingly rich, and gives good agreement with experiment when empirical relations for turbulent wall friction are included.

Keywords: Venturi; Bernoulli; Pump; Atomization

1. Introduction

Gas flowing from porous rock into a gas well is often accompanied by liquid. The gas flows to the earth's surface, and sufficiently small liquid droplets will be carried upwards by the gas. Larger droplets sediment under gravity to the bottom of the well, where the liquid level rises slowly.

* Corresponding author. Tel.: +44 1223 325363; fax: +44 1223 467004.
E-mail address: sherwood@cambridge.oilfield.slb.com (J.D. Sherwood).

0301-9322/$ - see front matter © 2004 Elsevier Ltd. All rights reserved.
doi:10.1016/j.ijmultiphaseflow.2004.08.006

Eventually the liquid may reach a gas-bearing rock stratum and block the flow of gas. Gas production is reduced or ceases altogether, and the well becomes uneconomic.

One way to prevent this is to pump liquid from the bottom of the well up to the surface by means of an electric submersible pump. Such a system is expensive to install and maintain, and may not be economic if the gas production of the well is small. Here we describe a device, based on a Venturi pump, which can atomize liquid and thereby suspend it in the main gas flow (Sherwood et al., 2003). The analysis is based on nothing more complicated than Bernoulli's equation and hydrostatic pressures, yet it predicts a rich variety of behaviour and appears to be qualitatively in agreement with the results of experiments described in Section 7. Quantitative agreement is surprisingly good when turbulent pressure losses are included in the analysis.

The very simplest form of the device is shown in Fig. 1. A Venturi is introduced into the main gas flow, and a region of low pressure p_G is created at the Venturi throat, from where a pipe GB descends to the liquid at the sump of the well, a distance $h = h_1 + h_2$ below the Venturi. The surface of the liquid is at a pressure p_B. If the liquid density is ρ_L and g is the acceleration due to gravity, liquid will start to flow up the pipe BG if the pressure difference $P = p_B - p_G$ can overcome the hydrostatic head, i.e. if

$$P = p_B - p_G > \rho_L g h = \rho_L g(h_1 + h_2). \tag{1}$$

The Venturi pump lifts and atomizes liquid, in much the same manner as does a simple perfume atomizer or a jet pump (Kay and Nedderman, 1974). However, if the gas flow rate is low, the pressure difference P generated by the Venturi may be insufficient to lift liquid the required height h. We cannot make h smaller by allowing the liquid level to rise within the well, since the pressure of

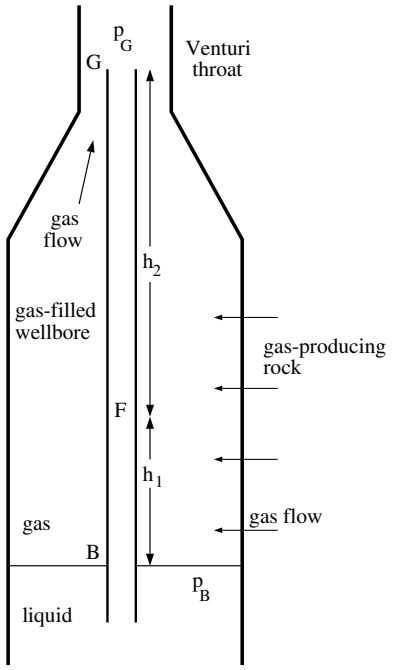

Fig. 1. The lift pressure $P = p_B - p_G$ is generated by a Venturi.

the gas within the rock pores is often low. Only a small hydrostatic head of liquid within the well suffices to block gas flow into the well from the pores of the surrounding rock. A rise in liquid level therefore reduces the gas flow rate within the well and hence reduces the differential pressure generated by the Venturi. Similarly, there is nothing to be gained by moving the Venturi below the top of the zone that produces gas. If liquid has risen to the bottom of the production zone, and gas production is uniform over the height of this zone, then the gas flow rate through a Venturi situated a distance h above the liquid would be proportional to h, and the Venturi differential pressure would vary as h^2, whereas the hydrostatic head that must be overcome is proportional to h. It is therefore advantageous to make h as large as possible.

One way to reduce the pressure required to overcome the hydrostatic head may be to introduce gas (of density $\rho_G < \rho_L$) into the vertical pipe BG at F, distance $h_1 < h$ above the surface of the liquid, so that the density of the gas–liquid mixture in the pipe FG is reduced to $\rho_3 < \rho_L$, with ρ_3 sufficiently small that

$$P > \rho_L g h_1 + \rho_3 g h_2. \tag{2}$$

The Venturi pump can thereby raise the low density gas–liquid mixture a greater height than it could pure liquid.

One might expect that it is best to make h_1 as small as possible, but we shall see in Section 3.4 that this is not always so. In addition, for practical reasons we would normally want to keep the gas inlet A (Fig. 2) well above the liquid surface B, the position of which may vary with time. The

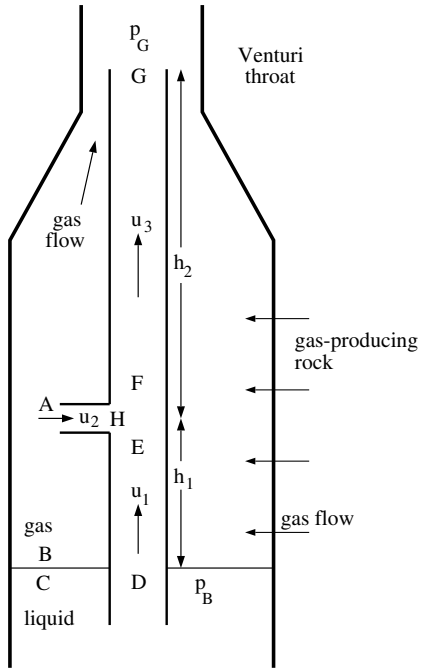

Fig. 2. As in Fig. 1, but gas now enters the main riser DG at H. The cross-sectional area of the main riser DG is A_1, and that of the gas inlet AH is A_2. The total height that liquid must be lifted is $h = h_1 + h_2$.

engineer who designs such a lifting device has only four variables that he can change in order to optimize the process: (i) the differential pressure P generated by the Venturi, which he can control by his choice of the Venturi throat diameter; (ii) the position h_1 of the gas inlet; (iii) the cross-sectional area A_2 of the gas inlet; and (iv) the cross-sectional area A_1 of the main vertical pipe.

Our aim is to predict the rate at which liquid is lifted as a function of the various geometrical factors and liquid properties. In Section 2 we use Bernoulli's equation and hydrostatic pressures to relate the various pressures and velocities within the device. Then in Section 3 we combine these relations in order to predict the flow rates. Zero liquid flow rate is dealt with in Section 3.1, and the equation predicting liquid flow rates when these are non-zero is obtained in Section 3.2. The simpler case $h_1 = 0$ is discussed in detail in Section 3.3, and the more general case $h_1 > 0$ is considered in Section 3.4. In Section 4 we show that allowing gas to enter the main riser at several points (rather than at just one) makes the positioning of the gas entrance less crucial, but reduces the efficiency of the device. Then in Section 5 we show that the lifting of liquid is achieved only at the cost of reduced pressures downstream of the Venturi.

We shall assume that the gas is incompressible: this approximation could be relaxed in a more complete model. In general we neglect any motion of gas relative to liquid, except in Section 6 where the effects of such relative motion are investigated in a simple fashion by allowing a constant relative velocity u_s between the two phases. The effects of viscosity and interfacial tension are assumed negligible. In particular, we assume that wall friction is negligibly small, except in Section 7 where turbulent wall friction will be considered when interpreting experimental results.

Some of the liquid atomized by the Venturi may subsequently contact the wellbore walls and form a thin liquid film which flows back downwards, so the lifting process may be inefficient and require several stages. We shall discuss only the initial lifting of liquid by the Venturi, and not the global problem of how much of the atomised liquid reaches the surface: this latter problem is more specific to the gas-well application which first generated our interest in Venturi atomizers. Methods for re-dispersing any liquid films that form on the wellbore walls are considered by Sherwood et al. (2003).

2. The pressures within the device

We consider the flow geometry shown in Fig. 2. The region CDE contains liquid of density ρ_L and the region ABH outside the device contains incompressible gas of density ρ_G. We assume that fluid flows in each pipe with a velocity which is uniform over the pipe cross-section, and we neglect the possibility that liquid flow in the lower vertical pipe DE may be laminar, with a consequent parabolic velocity profile.

The main pipe DEFG has cross-sectional area A_1 and the liquid velocity in the lower pipe DE is u_1. The gas velocity is u_2 in the inlet pipe H, which has area A_2. Conservation of volume implies that the velocity in the upper section of pipe GF must be

$$u_3 = u_1 + u_2 a_2, \tag{3}$$

where

$$a_2 = A_2/A_1 \tag{4}$$

and the density of the gas–liquid mixture in the upper pipe is

$$\rho_3 = \frac{\rho_G u_2 A_2 + \rho_L u_1 A_1}{u_1 A_1 + u_2 A_2} = \frac{\rho_G u_2 a_2 + \rho_L u_1}{u_1 + u_2 a_2}. \tag{5}$$

If we allow relative motion between liquid and gas in GE, Eqs. (3) and (5) require modification, as discussed in Section 6.

The pressure at B and C is p_B. By Bernoulli's equation, in the absence of losses the pressure at D is

$$p_D = p_B - \frac{1}{2}\rho_L u_1^2. \tag{6}$$

More realistically, the pressure at D will be lower than predicted by Bernoulli, due to entry pressure losses. These losses are often expressed in the form $\frac{1}{2}K\rho_L u_1^2$, with $K \approx 0.6$ for an abrupt contraction, though this can easily be reduced to $K < 0.1$ by suitable machining of a smooth entrance (Miller, 1978); we shall ignore such losses. In the absence of wall friction the pressures at A and F are

$$p_A = p_B - \rho_G h_1 g, \tag{7}$$

$$p_F = p_G + \rho_3 h_2 g. \tag{8}$$

If the tube DE is filled with liquid, then

$$p_E = p_D - \rho_L h_1 g = p_B - \frac{1}{2}\rho_L u_1^2 - \rho_L g h_1. \tag{9}$$

If instead the tube DE is filled with liquid only to a height h_3, with $u_1 = 0$, then

$$p_E = p_D - \rho_L h_3 g - \rho_G (h_1 - h_3) g = p_B - \rho_L g h_3 - \rho_G (h_1 - h_3) g. \tag{10}$$

By Bernoulli's equation, the pressure at H is

$$p_H = p_A - \frac{1}{2}\rho_G u_2^2 = p_B - \rho_G h_1 g - \frac{1}{2}\rho_G u_2^2, \tag{11}$$

where again, as in (6), entry losses have been neglected.

We assume that viscous effects are negligible, and consider the momentum integral (Batchelor, 1967, Eq. 3.2.3) in the vertical (z) direction over a control volume JKML shown in Fig. 3. This leads to

$$p_E - p_F = \rho_3 u_3^2 - \rho_L u_1^2 = \rho_L u_1 (u_3 - u_1) + \rho_G u_2 u_3 a_2 = u_1 u_2 a_2 (\rho_L + \rho_G) + \rho_G u_2^2 a_2^2, \tag{12}$$

where we have assumed that there is no relative velocity between gas and liquid, and that the pressure is uniform over cross-sections JFK and MEL of the pipe. This latter approximation can be more reasonably justified by using a larger control volume than that shown in Fig. 3, with JFK and MEL positioned further downstream and upstream, respectively.

It is less obvious how to apply the momentum equation (over the same control volume) in the horizontal (x) direction. The x momentum of gas coming from the inlet JM must be destroyed,

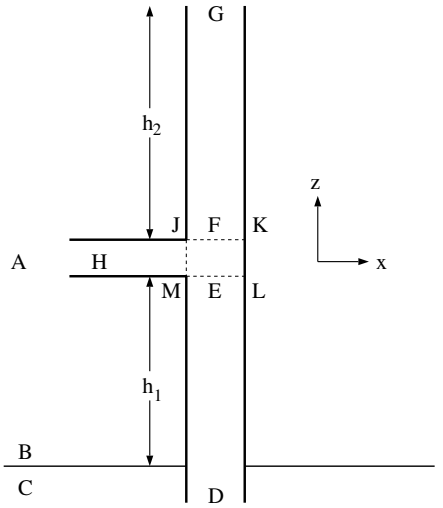

Fig. 3. Detailed geometry of the junction at which gas enters the main riser.

but if the force required to do this is spread over a large area of pipe wall opposite the entrance, the increase in pressure will be negligibly small. We shall therefore neglect this increase. One option at this point would be to assume that the gas pressure at the inlet JM is equal to the average pressure within the pipe, with $p_H = \frac{1}{2}(p_E + p_F)$. However, this leads to inconsistencies when $u_1 = 0$. Since it is important to be able to predict when liquid reaches the junction at E, we shall instead assume

$$p_H = p_E \tag{13}$$

so that if $u_1 > 0$, by (9), (11) and (13),

$$\rho_G h_1 g + \frac{1}{2}\rho_G u_2^2 = \rho_L h_1 g + \frac{1}{2}\rho_L u_1^2, \quad u_1 > 0. \tag{14}$$

If the pressure in the Venturi throat is insufficiently low, liquid will only be lifted a distance $h_3 < h_1$ up the lower section DE of the riser, and $u_1 = 0$, so that (10) holds, rather than (9). Instead of (14) we find that the liquid level h_3 is given by

$$(\rho_L - \rho_G) h_3 g = \frac{1}{2}\rho_G u_2^2, \quad u_1 = 0. \tag{15}$$

An initial investigation assumed $p_H = \frac{1}{2}(p_E + p_F)$, rather than (13). Results were very similar to those presented below, though the algebra was considerably more involved.

3. Solving the governing equations

We now combine the equations obtained in the previous section in order to investigate the operation of the device.

3.1. Zero liquid flow, $u_1 = 0$

If the pressure generated by the Venturi is insufficient to pump liquid, the device fails. Nevertheless, we first discuss this case in order to examine the gas flow predicted by the model.

The liquid velocity $u_L = 0$ and there is only gas in the upper section of the main riser, so that $\rho_3 = \rho_G$. From (12), (8), (11) and (13) we obtain

$$p_B - p_G = \rho_G g(h_1 + h_2) + \frac{1}{2}\rho_G u_2^2 + \rho_G u_2^2 a_2^2. \tag{16}$$

In this case we see that the pressure drop consists of a hydrostatic head, together with a pressure drop $\frac{1}{2}\rho_G u_2^2$ at the gas entry A (which is not recovered when gas emerges into the main riser from the inlet H), and a pressure loss $\rho_G u_2^2 a_2^2$ required to give the gas its momentum in the vertical direction. This last term is negligible when $a_2 \ll 1$. However, if $a_2 = 1$ the pressure drop at the T-junction appears excessive, suggesting that any design based upon these equations will be conservative.

If the diameter of the wellbore is d_w and that of the Venturi throat is βd_w, and the velocity of gas within the Venturi throat is u_{GV}, then the main gas flow is subjected to a pressure drop

$$\Delta P = \frac{1}{2}\rho_G u_{GV}^2(1 - \beta^4) \tag{17}$$

as it flows into the throat of the Venturi. Adding to (17) the hydrostatic pressure drop in the gas-filled well we obtain

$$p_B - p_G = \frac{1}{2}\rho_G u_{GV}^2(1 - \beta^4) + \rho_G g(h_1 + h_2). \tag{18}$$

Comparing (16) and (18) we conclude that when $a_2 \ll 1$ and $\beta \ll 1$ then in the absence of liquid (i.e. if $u_1 = 0$) the velocity u_2 of gas in the inlet pipe is the same as the gas velocity u_{GV} in the Venturi throat. The gas velocity $u_3 = u_2 a_2$ in the main riser FG is therefore smaller than that in the Venturi throat by a factor a_2.

3.2. The governing equations when $u_1 > 0$

Our main interest is in a device for which $u_1 > 0$ so that liquid is pumped up to the Venturi throat. We now combine the equations derived in Section 2 in order to obtain an equation giving the velocity u_1 at which liquid is raised in terms of the pressure difference $P = p_B - p_G$ available for lifting liquid.

In this case, by (12), (8) and (9),

$$p_B - p_G = u_1 u_2 a_2(\rho_L + \rho_G) + \rho_G u_2^2 a_2^2 + \frac{1}{2}\rho_L u_1^2 + \rho_L g h_1 + \rho_3 h_2 g. \tag{19}$$

We can eliminate ρ_3 from (19) by means of (5), but in order to simplify the analysis we assume that $\rho_G \ll \rho_L$ in terms associated with hydrostatic pressures (but *not* in terms associated with inertia, since gas velocities may be high). Hence (19) becomes

$$P = p_B - p_G = u_1 u_2 a_2(\rho_L + \rho_G) + \frac{1}{2}\rho_L u_1^2(1 + 2a_2^2) + (1 + 2a_2^2)\rho_L g h_1 + \frac{h_2 g \rho_L u_1}{u_1 + u_2 a_2} \tag{20}$$

and by (14)

$$\rho_G u_2^2 = \rho_L u_1^2 + 2\rho_L h_1 g \tag{21}$$

so that

$$u_2 = u_1 \left(\frac{\rho_L}{\rho_G}\right)^{1/2} S, \tag{22}$$

where

$$S = \left(1 + \frac{2h_1 g}{u_1^2}\right)^{1/2}. \tag{23}$$

Hence the velocity in the main riser is

$$u_3 = u_1 + a_2 u_2 = u_1(1 + bS), \tag{24}$$

where

$$b = a_2(\rho_L/\rho_G)^{1/2}. \tag{25}$$

The liquid volume fraction ϕ_L in the main riser is

$$\phi_L = \frac{u_1}{u_1 + u_2 a_2} = \frac{1}{1 + bS}. \tag{26}$$

We non-dimensionalize velocities by $(2P/\rho_L)^{1/2}$ such that the non-dimensional liquid velocity is

$$\hat{u}_1 = u_1 \left(\frac{\rho_L}{2P}\right)^{1/2} \tag{27}$$

and we set

$$G = \frac{h_2 g \rho_L}{P}, \quad \hat{h}_1 = h_1/h_2. \tag{28}$$

$G = 1$ corresponds to the case in which the pressure P would be just capable of lifting liquid a distance h_2.

Eliminating u_2 from (20) by means of (21) we obtain

$$P = \frac{u_1^2 \rho_L}{2}\left\{1 + 2a_2^2 + 2b[1 + \rho_G/\rho_L]S\right\} + (1 + 2a_2^2)\rho_L g h_1 + \frac{h_2 g \rho_L}{1 + bS}. \tag{29}$$

We assume that $a_2 \ll 1$, but $\rho_L \gg \rho_G$ and so $b = a_2(\rho_L/\rho_G)^{1/2}$ is not negligible. Eq. (29) simplifies to

$$P = \frac{u_1^2 \rho_L}{2}(1 + 2bS) + \rho_L g h_1 + \frac{h_2 g \rho_L}{1 + bS} \tag{30}$$

or in non-dimensional form

$$1 = \hat{u}_1^2(1 + 2bS) + G\hat{h}_1 + \frac{G}{1 + bS}, \tag{31}$$

where, by (23)

$$S = \left(1 + \frac{G\hat{h}_1}{\hat{u}_1^2}\right)^{1/2}. \tag{32}$$

Eq. (31) gives us the non-dimensional liquid velocity $\hat{u}_1$ as a function of the non-dimensional pressure G^{-1} and position $\hat{h}_1$ at which gas enters, and is the key equation that we have been seeking. Once u_1 is known, the cross-sectional area A_1 of the main riser can be chosen such that liquid volumetric flowrate $q_L = u_1 A_1$ of the device exceeds the rate Q_L at which liquid is entering the well.

We now investigate (31) in more detail, first (Section 3.3) when $h_1 = 0$, and then (Section 3.4) for $h_1 > 0$.

3.3. The case $h_1 = 0$

We now assume $h_1 = 0$, since one might intuitively expect that there is little point in putting the gas entry higher than it need be. Eq. (31) becomes

$$1 = \hat{u}_1^2(1 + 2b) + \frac{G}{1 + b} \tag{33}$$

so that

$$\hat{u}_1^2 = \frac{b - G + 1}{(1 + b)(1 + 2b)}. \tag{34}$$

We now investigate the effect of changing b at fixed G (i.e. at a fixed differential pressure P). Fig. 4 shows the liquid velocity $\hat{u}_1$ as a function of b, for various G. There are solutions of (33) only if $G < b + 1$. Thus if b is small (corresponding to injection of only a small amount of gas) the device will operate only if $G - 1$ is small. If we make b very large (while keeping $a_2 \ll 1$) there is a solution of (33) with

$$\hat{u}_1^2 \approx (1 + 2b)^{-1}, \quad \phi_L = (1 + b)^{-1} \ll 1. \tag{35}$$

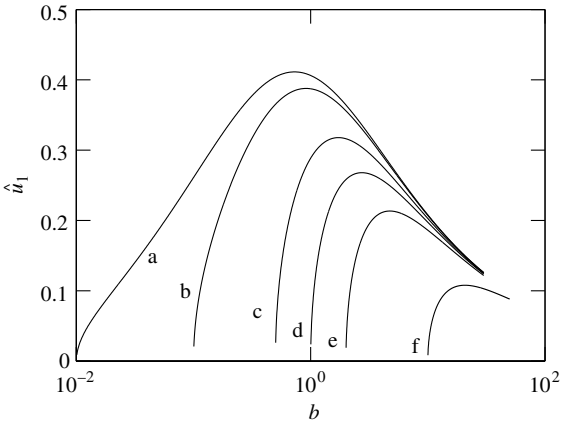

Fig. 4. The non-dimensional liquid velocity $\hat{u}_1 = u_1(\rho_L/2P)^{1/2}$ as a function of scaled gas inlet area $b = a_2(\rho_L/\rho_G)^{1/2}$. (a) $G = 1.01$, (b) $G = 1.1$, (c) $G = 1.5$, (d) $G = 2.0$, (e) $G = 3$, and (f) $G = 11$.

We note from Fig. 4 that for any given G there is an optimal $b = b_m$ such that u_1 is maximised. Differentiation of (33) gives

$$b_m = G - 1 + \left(G^2 - \frac{G}{2}\right)^{1/2}. \tag{36}$$

The maximum values of $\hat{u}_1^2$ when $b = b_m$ are shown in Fig. 5 (curve a). In the limit $G \to \infty$ we find

$$b_m \sim 2G, \quad \hat{u}_1^2 \sim \frac{1}{8G}. \tag{37}$$

Note that $b_m = 2^{-1/2}$ when $G = 1$. If $G < 1$ the Venturi could lift liquid without any assistance from gas, and the liquid velocity predicted by Bernoulli would be simply

$$\hat{u}_1^2 = 1 - G. \tag{38}$$

This velocity is also shown in Fig. 5 (curve b), and is tangent to the optimal results with gas (curve a) at $G = \frac{2}{3}$ which corresponds to $b = 0$. From (36) we see that $b_m < 0$ when $G < \frac{2}{3}$, and so we reject the corresponding part of curve (a) of Fig. 5 as unphysical.

3.4. The case $h_1 > 0$

We consider next the more general case $h_1 > 0$. If the volumetric flow rate Q_{LW} of liquid entering the well is greater than the rate $Q_L = u_1 A_1$ at which liquid is lifted by the Venturi pump, the level of liquid at the base of the well will rise. Lifting will eventually cease when the gas inlet is flooded with liquid. On the other hand, if $Q_{LW} < A_1 u_1$ the liquid level will fall and the distance h_1 will increase. Clearly we require that as h_1 decreases the liquid velocity u_1 increases sufficiently rapidly for the pump rate $u_1 A_1$ to match the inflow rate Q_{LW} before $h_1 = 0$ and the device is flooded.

Numerical solutions of (31) are shown in Figs. 6–12. In the limit $\rho_L g h_1 = P$ the pressure P is only just able to lift liquid to the point of gas entry, and we note from (31) that $\hat{u}_1 \to 0$ as $Gh_1/h_2 \to 1$. We can therefore find solutions to (31) only if

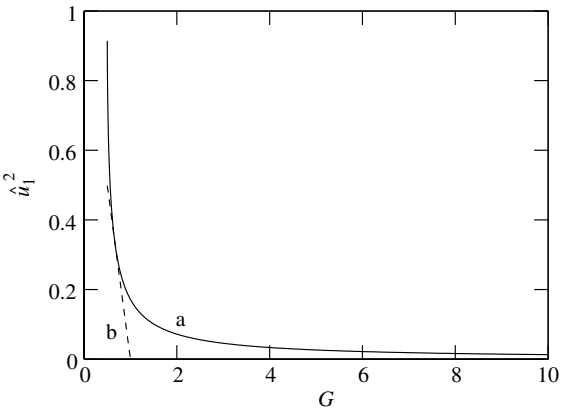

Fig. 5. (a) The maximal values of $\hat{u}_1^2$, given by (34) when $b = b_m$ (36). (b) $\hat{u}_1^2$, given by (38) in the absence of gas.

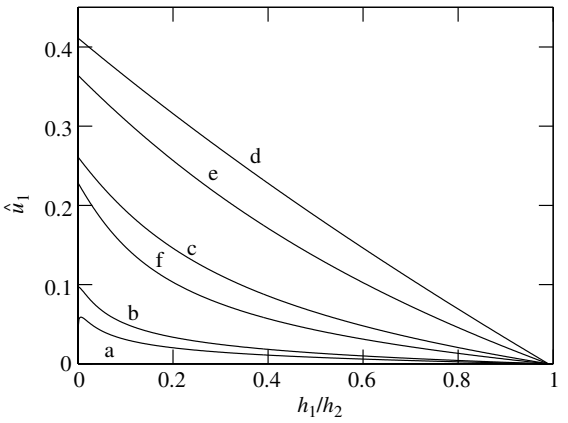

Fig. 6. $\hat{u}_1$ as a function of h_1/h_2, for $G = 1.01$. (a) $b = 0.012$, (b) $b = 0.02$, (c) $b = 0.1$, (d) $b = b_m = 0.7277$, (e) $b = 2.0$, and (f) $b = 8.0$.

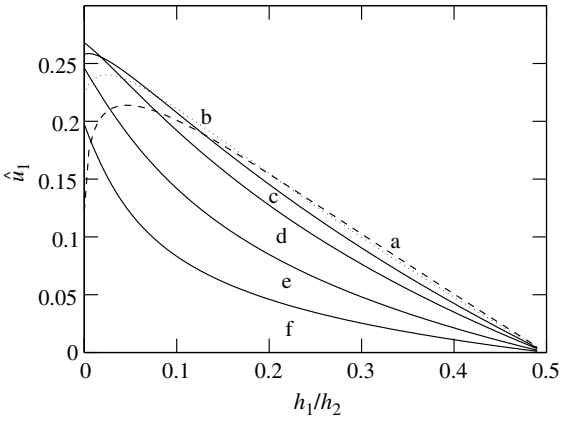

Fig. 7. $\hat{u}_1$ as a function of h_1/h_2, for $G = 2.0$. (a) $b = 1.1$, (b) $b = 1.5$, (c) $b = 2.0$, (d) $b = b_m = 2.73$, (e) $b = 5.0$, and (f) $b = 10.0$.

$$P > h_1 g \rho_L, \tag{39}$$

i.e. if

$$\frac{h_1}{h_2} < G^{-1}. \tag{40}$$

Fig. 6 shows the liquid velocity $\hat{u}_1$ for various values of b when $G = 1.01$. The results of the previous section correspond to $h_1 = 0$ i.e. to results on the left-hand axis of Fig. 6. We see that the liquid velocity u_1 increases as b increases to $b = b_m = 0.7277$, and then decreases for $b > b_m$, as predicted in Section 3.3.

In general, for fixed b the liquid velocity decreases as h_1 increases, as is required for a stable equilibrium to be possible. However, we can just observe on curve (a) of Fig. 6 a region close

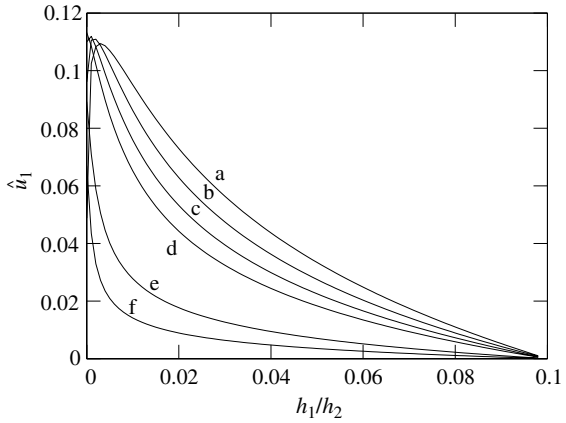

Fig. 8. $\hat{u}_1$ as a function of h_1/h_2, for $G = 10.0$. (a) $b = 9.5$, (b) $b = 12.0$, (c) $b = 15.0$, (d) $b = b_m = 18.74$, (e) $b = 50.0$, and (f) $b = 100.0$.

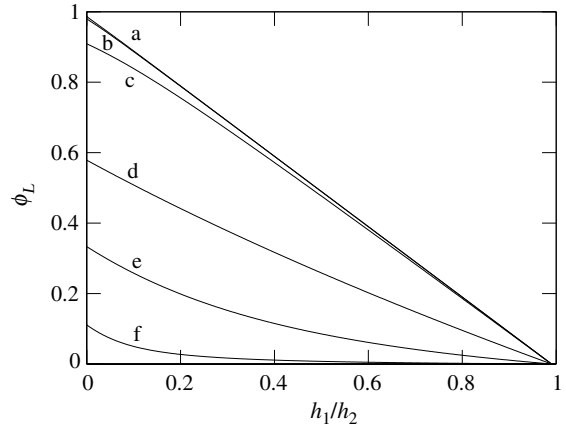

Fig. 9. The liquid volume fraction ϕ_L in the riser FG, for the case corresponding to Fig. 6. $G = 1.01$; (a) $b = 0.012$, (b) $b = 0.02$, (c) $b = 0.1$, (d) $b = b_m = 0.7277$, (e) $b = 2.0$, and (f) $b = 8.0$.

to $h_1 = 0$ where u_1 *increases* with h_1, and there is a value of h_1 for which u_1 attains a maximum. This is much clearer on Fig. 7 ($G = 2$) and Fig. 8 ($G = 10$). We now investigate the location of this maximum.

In the limit $h_1 \ll h_2$, then if $\hat{u}_1^2 \gg Gh_1/h_2$ the governing Eq. (31) can be expanded as

$$\hat{u}_1^2 = \frac{1+b-G}{(1+b)(1+2b)} - \frac{Gh_1}{h_2}\left[\frac{1+b}{1+2b} - \frac{Gb}{2(1+b)(1+b-G)}\right] + \mathrm{O}\left(\frac{h_1}{h_2}\right)^2. \tag{41}$$

The velocity $\hat{u}_1$ only decreases as h_1 increases if

$$G < G_1 = \frac{2(1+b)^3}{4b^2+5b+2} = 1 + \frac{b}{2} - \frac{b^2}{2(4b^2+5b+2)} < 1 + \frac{b}{2}. \tag{42}$$

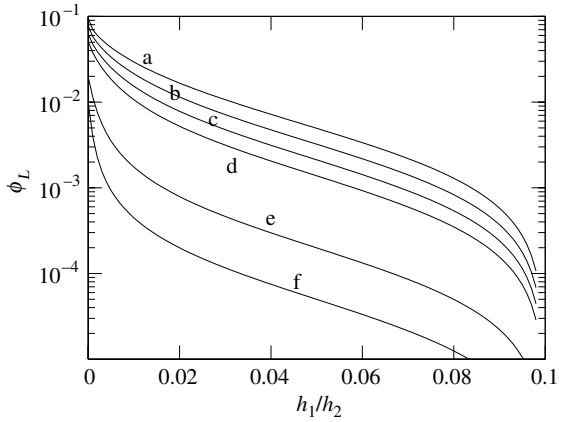

Fig. 10. The liquid volume fraction ϕ_L in the riser FG, for the case corresponding to Fig. 8. $G = 10.0$; (a) $b = 9.5$, (b) $b = 12.0$, (c) $b = 15.0$, (d) $b = b_m = 18.74$, (e) $b = 50.0$, and (f) $b = 100.0$.

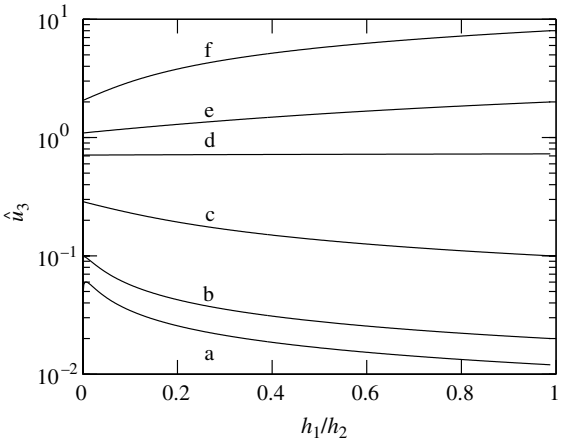

Fig. 11. The mixture velocity $\hat{u}_3$ in the riser FG, for the case corresponding to Figs. 6 and 9. $G = 1.01$; (a) $b = 0.012$, (b) $b = 0.02$, (c) $b = 0.1$, (d) $b = b_m = 0.7277$, (e) $b = 2.0$, and (f) $b = 8.0$.

We conclude that there are solutions with $u_1 > 0$ for which u_1 increases with h_1 in a neighbourhood of $h_1 = 0$ if

$$G_1 < G < 1 + b. \tag{43}$$

However, from (42) we see that G_1 is closely approximated by $1 + b/2$, and so to a close approximation (43) predicts that u_1 increases with h_1 near $h_1 = 0$ if

$$G - 1 < b \lessapprox 2(G - 1). \tag{44}$$

This agrees with the results presented in Figs. 6–8.

At first sight it seems surprising that when (42) does not hold, an increase in h_1 (i.e. an increase in the total height that the liquid must be raised) leads to an increase in the liquid flow rate. But in

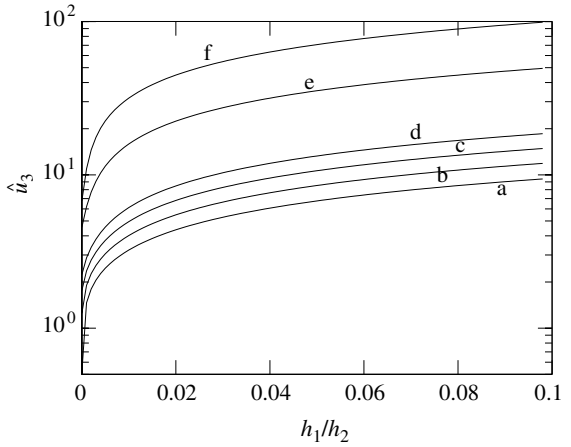

Fig. 12. The mixture velocity $\hat{u}_3$ in the riser FG, for the case corresponding to Figs. 8 and 10. $G = 10.0$; (a) $b = 9.5$, (b) $b = 12.0$, (c) $b = 15.0$, (d) $b = b_m = 18.74$, (e) $b = 50.0$, and (f) $b = 100.0$.

this case the flow rate of liquid is small. When h_1 is increased the pressure at the gas entry F is decreased and by (21) the total flow rate of gas increases. Consequently the gas fraction in the main riser FG is increased, and the hydrostatic pressure drop along FG is reduced. This would seem to more than cancel the effect of the increased hydrostatic pressure $\rho_L h_1 g$.

We can also make analytic progress in the limit $G \gg 1$. Differentiating (31) with respect to $\hat{h}_1$ we find

$$\frac{\mathrm{d}\hat{u}_1^2}{\mathrm{d}\hat{h}_1}\left[\frac{2b\hat{h}_1 G}{\hat{u}_1^2 S} - 2 - 4bS - \frac{G^2\hat{h}_1 b}{\hat{u}_1^4 S(1+bS)^2}\right] = \frac{2bG}{S} + 2G - \frac{G^2 b}{S(1+bS)^2\hat{u}_1^2}. \tag{45}$$

The liquid velocity $\hat{u}_1$ is non-zero if $G - 1 < b$ and is monotonic decreasing if $G - 1 \lessapprox b/2$. We therefore expect a maximum in $\hat{u}_1^2$ as a function of $\hat{h}_1$ if

$$b = \gamma G, \quad 1 \leqslant \gamma \leqslant 2, \quad G \gg 1 \tag{46}$$

and a maximum can be found if the scalings

$$\hat{h}_1 \sim \frac{\alpha}{2G^2}, \quad \hat{u}_1^2 \sim \frac{\delta}{2G} \tag{47}$$

hold, for some unknown α, γ and δ. From (31) and (45) we find $\delta = \frac{1}{4}$, so that the maximum velocity scales as

$$\hat{u}_1^2 \sim \frac{1}{8G}. \tag{48}$$

This is the same as the maximum velocity (37) when $h_1 = 0$. We have only two equations, (31) and (45), for α, δ and γ, and so we cannot hope to solve for all three unknowns. All we can say about γ and α is

$$1 + 4\alpha = 4\gamma^{-2}. \tag{49}$$

The bounds on γ are such that $0 < \alpha < \frac{3}{4}$. Thus there is a range of values of b which all lead to a similar maximum velocity, as can be seen in Fig. 8. We wish the device to operate with h_1 sufficiently large that the flow rate decreases as h_1 increases, i.e. in the region of Fig. 8 to the right of the maxima. We conclude from Fig. 8 that it is advantageous to make b as small as possible, subject to the requirement $b > G - 1$.

Figs. 9 and 10 show the liquid volume fractions ϕ_L in the riser FG corresponding to the cases considered in Figs. 6 and 8, and Figs. 11 and 12 show the corresponding mixture velocities $\hat{u}_3$ in the riser FG. When $G = 1.01$ and $b \ll 1$ the first term on the right-hand side of (31) is small, and so

$$\phi_L = \frac{1}{1 + bS} \approx \frac{1}{G} - \frac{h_1}{h_2}. \tag{50}$$

We see in Fig. 9 that ϕ_L does indeed vary linearly with h_1/h_2. This is not so in the case $G = 10$ considered in Fig. 10, since the requirement $b > G - 1$ ensures that the first term on the right-hand side of (31) can no longer be neglected when $G \gg 1$.

As $h_1/h_2 \to G^{-1}$ so $\phi_L \to 0$ and hydrostatic pressures in the main riser become negligible. If we assume that a_2 is sufficiently small that we may neglect the pressure $\frac{1}{2}\rho_G u_2^2 a_2^2$ associated with the gas velocity in the main riser, then in the absence of liquid we expect, from (16), $\frac{1}{2}\rho_G u_2^2 = P$ so that in the main riser

$$u_3 = a_2 u_2 = a_2 (2P/\rho_G)^{1/2}, \tag{51}$$

i.e.

$$\hat{u}_3 = b \tag{52}$$

and we see in Figs. 11 and 12 that this limit is approached as h_1/h_2 tends to the maximum value (40) for which liquid is lifted.

4. The effect of multiple holes for gas entry

If the gas entry hole H is placed too low on the riser (Fig. 2), it would be submerged if the liquid level were to rise too far. Gas entry would be prevented and the device would no longer work. We now consider whether we could replace this one hole by several holes, distributed along the length of the riser. This would make the positioning of the holes less critical.

We consider a device with just two holes, as shown in Fig. 13. We look to see whether gas flow can lift liquid to the level of the lower hole. We shall not investigate flow rates should the differential pressure be greater than the minimum required for flow just to occur.

Gas enters at the two side ports with no vertical momentum and as in Section 2 the pressure of the gas at entry is assumed equal to the pressure in the main riser just below the point of entry. We assume that the external pressure p_0 is the same for both side entry ports (i.e. hydrostatic pressures due to gas density are negligible). The cross-sectional area of the main vertical riser is A_1, and the areas of the gas inlets are $A_3 = a_3 A_1$ and $A_2 = a_2 A_1$.

By Bernoulli, at the entry into the upper port

$$p_2 + \frac{1}{2}\rho_G u_2^2 = p_0, \tag{53}$$

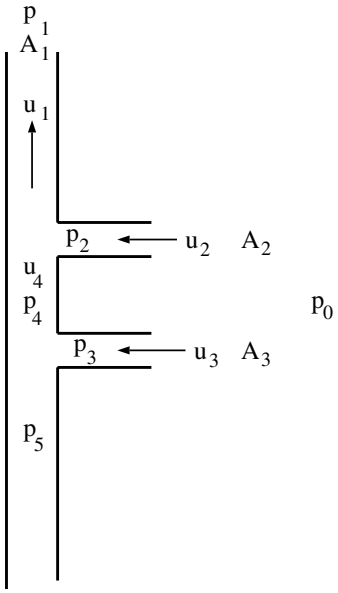

Fig. 13. A device with two holes for gas entry.

and at the entry into the lower port

$$p_3 + \frac{1}{2}\rho_G u_3^2 = p_0. \tag{54}$$

The pressure above the column of liquid is assumed to be equal to that in the lower gas entry, and is therefore $p_5 = p_3$. This is lower than p_0 as long as $u_3 > 0$. The device will only operate if the pressure difference $p_0 - p_5$ is sufficient to lift liquid to the lower of the two gas entry ports. We now show that $p_0 - p_5$ is smaller than the total pressure difference $p_0 - p_1$ generated by the Venturi, and that it is reduced even further by the presence of the additional gas entry port.

The velocity of gas up the main riser is

$$u_4 = u_3 A_3 / A_1 = u_3 a_3 \tag{55}$$

just above the lower inlet, and

$$u_1 = A_1^{-1}[u_3 A_3 + u_2 A_2] = u_3 a_3 + u_2 a_2 \tag{56}$$

in the upper section of the main riser. The vertical component of the integral form of the momentum equation gives

$$p_5 - p_4 = \rho_G u_4^2, \tag{57}$$

at the lower gas inlet, and, at the upper inlet

$$p_4 - p_1 = \rho_G u_4(u_1 - u_4) + \rho_G u_2 a_2 u_1 = \rho_G[2u_3 a_3 u_2 a_2 + (u_2 a_2)^2]. \tag{58}$$

We now eliminate velocities in order to obtain an expression for the pressure p_5 lifting the liquid in terms of the pressure p_1 generated by the Venturi. From (57), (55) and (54)

$$p_5 = p_4 + \rho_G u_3^2 a_3^2 = p_4 + 2(p_0 - p_3)a_3^2. \tag{59}$$

But we have assumed $p_5 = p_3$ and so

$$p_5 - p_0 = \frac{p_4 - p_0}{1 + 2a_3^2}. \tag{60}$$

From (58), (53) and (54)

$$p_4 - p_1 = 4a_2 a_3 (p_0 - p_2)^{1/2}(p_0 - p_3)^{1/2} + 2a_2^2(p_0 - p_2). \tag{61}$$

Setting $p_3 = p_5$, $p_2 = p_4$ and using (60) leads to

$$(p_0 - p_5)\left[4a_2 a_3 (1 + 2a_3^2)^{1/2} + (1 + 2a_2^2)(1 + 2a_3^2)\right] = p_0 - p_1. \tag{62}$$

This is the key relation which relates the pressure difference $p_0 - p_5$ (which lifts liquid), to the pressure difference $p_0 - p_1$ generated by the Venturi. If $a_2 = 0$ only one hole is open, and

$$p_0 - p_5 = \frac{p_0 - p_1}{1 + 2a_3^2}. \tag{63}$$

If $a_3 = 1$ then $p_0 - p_5 = (p_0 - p_1)/3$.

Suppose now that both holes are open, with $a_2 = a_3$, so that, by (62)

$$p_0 - p_5 = \frac{p_0 - p_1}{(1 + 2a_2^2)^2 + 4a_2^2(1 + 2a_3^2)^{1/2}}. \tag{64}$$

If $a_2 = a_1 = 1$ this is $p_0 - p_5 = (p_0 - p_1)/(9 + 4\sqrt{3}) \approx 0.063(p_0 - p_1)$, which is much smaller than the pressure $p_0 - p_5 = (p_0 - p_1)/3$ available to lift liquid when there is only one hole. The additional hole higher up the riser has reduced the extent to which the low pressure p_1 in the Venturi throat is able to influence the pressure p_5 at the surface of the liquid.

If both $a_2 \ll 1$ and $a_3 \ll 1$ then by (62)

$$p_0 - p_5 = (p_0 - p_1)[1 - 2(a_3 + a_2)^2] + \mathrm{O}(a^4), \tag{65}$$

and by extension we conclude that if gas is allowed to enter through many holes, the sum of their areas must be small compared to that of the main riser if $p_0 - p_5$ is not to become small compared to the Venturi differential pressure $p_0 - p_1$.

We can look at the amount of gas entering the two inlets. By (54)

$$\rho_G u_3^2 = 2(p_0 - p_3) = 2(p_0 - p_5). \tag{66}$$

By (53) and (60)

$$\rho_G u_2^2 = 2(p_0 - p_2) = 2(p_0 - p_4) = 2(p_0 - p_5)(1 + 2a_3^2). \tag{67}$$

Hence

$$u_2 = u_3(1 + 2a_3^2)^{1/2} \geqslant u_3. \tag{68}$$

Thus we see that additional holes tend to reduce the pressure available for lifting liquid. However, we saw in Section 3 that if the hole is too small a larger hole will increase the amount of liquid that is lifted, and under such circumstances there might be an advantage to be gained by allowing additional gas to enter through additional holes.

5. Pressure losses

The Venturi mixing device lifts and accelerates liquid. This requires energy, which must be supplied by the main gas flow, and we now investigate the consequent reduction in pressure downstream of the Venturi. As usual, we neglect any frictional losses, either at the walls of the device or losses caused by drag forces acting between liquid droplets and gas. We also assume that the loss coefficient of the Venturi is unity in single phase flow i.e. that there are no losses caused by separation from the Venturi walls in the diverging section. We return to the case of gas entry at a single hole, as shown in Fig. 2.

In the riser, the mixture velocity is u_3, so that the volumetric flow rate of liquid is

$$Q_{\mathrm{L}} = A_1 u_3 \phi_{\mathrm{L}} \tag{69}$$

and that of the gas is

$$Q_{\mathrm{Gr}} = A_1 u_3 (1 - \phi_{\mathrm{L}}). \tag{70}$$

The total volumetric flow rate of gas is Q_{G}, of which Q_{Gr} flows through the riser and

$$Q_{\mathrm{Gw}} = Q_{\mathrm{G}} - Q_{\mathrm{Gr}} \tag{71}$$

reaches the Venturi directly through the wellbore. The cross-sectional area of the wellbore is A_{w} and that of the Venturi throat is $A_{\mathrm{throat}} = \beta^2 A_{\mathrm{w}}$. The gas velocity in the wellbore just below the Venturi is

$$v_1 = Q_{\mathrm{Gw}}/A_{\mathrm{w}} \tag{72}$$

and the pressure here is p_1.

We assume that the Venturi throat is long, and that the gas/liquid mixture, introduced at the throat, has time to speed up to the velocity of the main gas flow before deceleration occurs in the diverging section. For the moment we assume that gas + liquid is injected into the Venturi throat perpendicular to the main flow, as shown in Fig. 14. The gas velocity in the throat upstream of the point of injection is

$$v_2 = \frac{Q_{\mathrm{Gw}}}{A_{\mathrm{throat}}} \tag{73}$$

and the pressure here is

$$p_2 = p_1 + \frac{\rho_{\mathrm{G}} Q_{\mathrm{Gw}}^2}{2}\left[\frac{1}{A_{\mathrm{w}}^2} - \frac{1}{A_{\mathrm{throat}}^2}\right]. \tag{74}$$

We assume that the gas/liquid mixture is at the same pressure p_2 when it enters the Venturi.

We now use the equation of continuity to evaluate the velocity v_4 of the combined liquid/gas mixture within the Venturi throat after mixing has occurred:

$$A_{\mathrm{throat}} v_4 = A_1 u_3 + Q_{\mathrm{Gw}} = Q_{\mathrm{G}} + Q_{\mathrm{L}}. \tag{75}$$

The integral form of the equation for momentum parallel to the axis of the Venturi gives

$$p_2 A_{\mathrm{throat}} + v_2 \rho_{\mathrm{G}} Q_{\mathrm{Gw}} = p_4 A_{\mathrm{throat}} + v_4 [Q_{\mathrm{G}} \rho_{\mathrm{G}} + Q_{\mathrm{L}} \rho_{\mathrm{L}}], \tag{76}$$

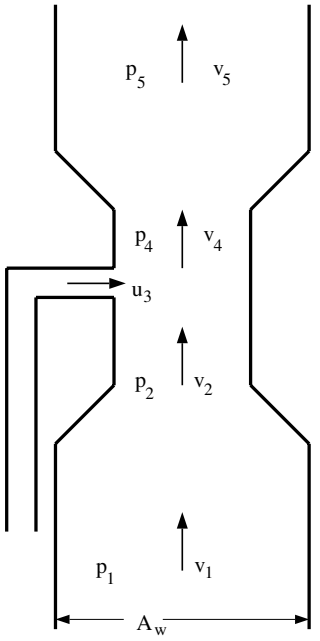

Fig. 14. Injection of the gas–liquid mixture from the riser into the Venturi throat, perpendicular to the main gas flow.

where the pressure downstream of the entry point is p_4. Since $v_4 > v_2$ it is clear that $p_4 < p_2$ and pressure has been lost.

The mixture slows down in the diverging section, and attains a velocity v_5, density ρ_5 and pressure p_5 in the straight section of wellbore above the Venturi, with

$$v_5 = \frac{Q_G + Q_L}{A_w}, \quad \rho_5 = \frac{Q_G\rho_G + Q_L\rho_L}{Q_G + Q_L}, \quad p_5 = p_4 + \frac{\rho_5}{2}(v_4^2 - v_5^2). \tag{77}$$

Hence, by (74), (76) and (77),

$$p_5 = p_1 - \frac{1}{2}\left(\frac{1}{A_{\text{throat}}^2} + \frac{1}{A_w^2}\right)\left[(Q_G + Q_L)(Q_G\rho_G + Q_L\rho_L) - \rho_G Q_{Gw}^2\right]. \tag{78}$$

In the absence of any flow in the riser, $Q_L = 0$ and $Q_{Gw} = Q_G$, and (78) predicts $p_1 = p_5$. If $\phi_L = 1$, so that there is no gas in the riser and $Q_G = Q_{Gw}$, then

$$p_5 = p_1 - \frac{1}{2}\left[\frac{1}{A_{\text{throat}}^2} + \frac{1}{A_w^2}\right](Q_G Q_L(\rho_G + \rho_L) + Q_L^2\rho_L). \tag{79}$$

More generally, we see from (78) that the pressure p_5 downstream of the Venturi is lower than that upstream, despite the assumed absence of viscous effects or other losses.

Alternatively, the main riser might discharge liquid in the direction of flow (as in Fig. 2). We omit details of the analysis, which is similar to that given above. In practice, the injection velocity u_3 and liquid volume fraction ϕ_L are such that the pressure downstream of the Venturi is lower than that upstream in this case also.

6. The effect of relative velocity between gas and liquid

In Sections 2–5 it has been assumed that the gas and liquid move at the same velocity. If the gas flows more quickly than liquid, then for given volumetric flow rates of gas and liquid the liquid holdup in the column will be increased, as will the density of the gas–liquid mixture. We might therefore expect the efficiency of the pump to be reduced, though the results presented below indicate that this is not always correct.

We adopt a simple model in which the steady upwards velocity u_L of liquid and the velocity u_G of gas differ by a constant relative velocity

$$u_s = u_G - u_L. \tag{80}$$

An obvious estimate for u_s in a tube of radius r could be based on the rise velocity of a Taylor bubble: $u_s = 0.48(gr)^{1/2}$ which, after non-dimensionalization becomes

$$\hat{u}_s = 0.48\left(\frac{gr\rho_L}{2P}\right)^{1/2}. \tag{81}$$

Such a choice is easiest to justify in slug flow. In the experiments the gas–liquid flow regime in the main riser was somewhere between slug and churn flow.

If u_L and $u_G = u_L + u_s$ are the velocities of gas and liquid in the upper portion FG of the main riser (Fig. 2), then

$$\phi_L u_L = u_1, \tag{82a}$$

$$(1-\phi_L)u_G = a_2 u_2, \tag{82b}$$

where the liquid volume fraction ϕ_L is obtained by eliminating u_L and u_G from (82):

$$\phi_L = \frac{-(u_1 + a_2u_2 - u_s) + \left[(u_1 + u_2a_2 - u_s)^2 + 4u_1u_s\right]^{1/2}}{2u_s}. \tag{83}$$

This leads, in the limit $u_s \to 0$, to

$$\phi_L \approx \frac{u_1}{u_1 + u_2a_2} + \frac{u_1u_2a_2u_s}{(u_1 + u_2a_2)^3} + O(u_s^2), \quad u_s \ll u_L. \tag{84}$$

The density of the gas–liquid mixture in the upper pipe is

$$\rho_3 = \rho_G(1-\phi_L) + \rho_L\phi_L \approx \rho_L\phi_L, \tag{85}$$

where, as usual, we neglect the gas density in hydrostatic pressures, even though it is important in Bernoulli's equation. The momentum equation in the vertical direction at the gas inlet (12) becomes

$$p_E - p_F = \rho_L u_1(u_L - u_1) + \rho_G u_2a_2u_G = \rho_L u_1(u_L - u_1) + \rho_G u_2a_2(u_L + u_s). \tag{86}$$

Combining (8), (9) and (86), the total pressure drop across the device is

$$\begin{aligned} P = p_B - p_G &= \rho_L u_1(u_L - u_1) + \rho_G u_2a_2u_G + \frac{1}{2}\rho_L u_1^2 + \rho_L g h_1 + \rho_L\phi_L h_2 g \\ &= \rho_L u_1^2(\phi_L^{-1} - 1) + \frac{\rho_G u_2^2a_2^2}{1-\phi_L} + \frac{1}{2}\rho_L u_1^2 + \rho_L g h_1 + \rho_L\phi_L h_2 g, \end{aligned} \tag{87}$$

which after non-dimensionalization using (27) and (28) becomes

$$1 = \hat{u}_1^2\left[2\phi_L^{-1} - 1 + \frac{2a_2^2S^2}{1-\phi_L}\right] + G\left(\frac{h_1}{h_2}\right) + G\phi_L. \tag{88}$$

In the limit $u_s \to 0$, ϕ_L is given by (26), so that the governing equation (88) reduces to (29). More generally, we may use (21) to eliminate u_2 from the expression (83) for the liquid density:

$$2\phi_L = 1 - x(1+bS) + \left[(1-x(1+bS))^2 + 4x\right]^{1/2}, \tag{89}$$

where $x = u_1/u_s = \hat{u}_1/\hat{u}_s$.

If we assume $a_2^2 \ll 1$, the governing equation (88) reduces to

$$1 = \hat{u}_1^2[2\phi_L^{-1} - 1] + G\left(\frac{h_1}{h_2}\right) + G\phi_L, \tag{90}$$

which in the limit $u_s \to 0$ reduces to (31).

The governing equation (90) can be solved by means of a Newton–Raphson iterative procedure. Typical results are plotted in Fig. 15 for the case $G = 2$, $b = 2.73$. The liquid velocity u_1 is reduced somewhat when $h_1 \ll h_2$ and the liquid volume fraction ϕ_L is large. Hydrostatic pressures are not negligible, and an increase in the liquid volume fraction reduces the pressure available to lift liquid. However, when h_1 becomes larger the liquid volume fraction becomes smaller and hydrostatic pressures are less important. Other things being equal, if the liquid velocity above the point of gas entry is reduced relative to the gas velocity, the inertial pressure required to accelerate the liquid becomes smaller. This reduction dominates the increase in hydrostatic pressure, and allows a minor increase in the liquid volumetric flow rate.

Results were found by an iterative technique, starting at $h_1 = 0$. At $h_1 = 0$ no solution could be found above some maximum relative velocity ($\hat{u}_s = 0.49$ when $b = 2.73$). This relative velocity may be compared to velocities in the absence of relative motion: if $\hat{u}_s = 0$, $G = 2$, $h_1 = 0$, then $\hat{u}_3 = 1.0$ when $b = 2.73$. No attempt was made to investigate the domain over which solutions could be found when $h_1 > 0$. In particular, for larger values of h_1, where velocities $\hat{u}_3$ are typically

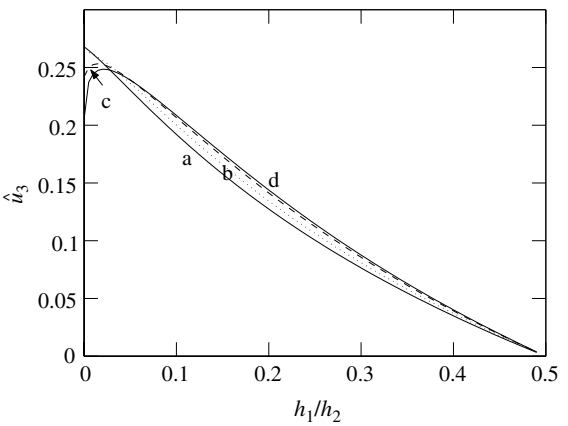

Fig. 15. $\hat{u}_1$ as a function of h_1/h_2, for $G = 2.0$, $b = 2.73$. (a) $\hat{u}_s = 0$, (b) $\hat{u}_s = 0.2$, (c) $\hat{u}_s = 0.4$, and (d) $\hat{u}_s = 0.48$.

larger, the predicted velocity $\hat{u}_1$ appears rather insensitive to $\hat{u}_s$ and there may be solutions for larger values of $\hat{u}_s$ than those shown in Fig. 15.

7. Experiments

In practice it is undesirable to block a wellbore any more than is necessary, so the design of Fig. 2, in which the main riser occupies part of the Venturi throat, is to be avoided. Fig. 16a shows an alternative configuration in which the Venturi is straight (minimizing pressure losses) but the riser does not enter the throat of the Venturi and therefore does not take advantage of the minimal pressure there. Fig. 16b shows the configuration adopted for the experiments presented here, which used a standard 3 in. ISO Venturi with diameter ratio $\beta = 0.455$. The main riser, of internal diameter $d_1 = 9\,\text{mm}$, turned through 30° before entering the Venturi throat via an aperture of length 46 mm. The large opening and gentle bend reduced pressure losses compared to those found with a sharp 90° bend. Further work could be done to modify the liquid injection in order to reduce the size of the aerosol droplets and improve their transport upwards in the main gas

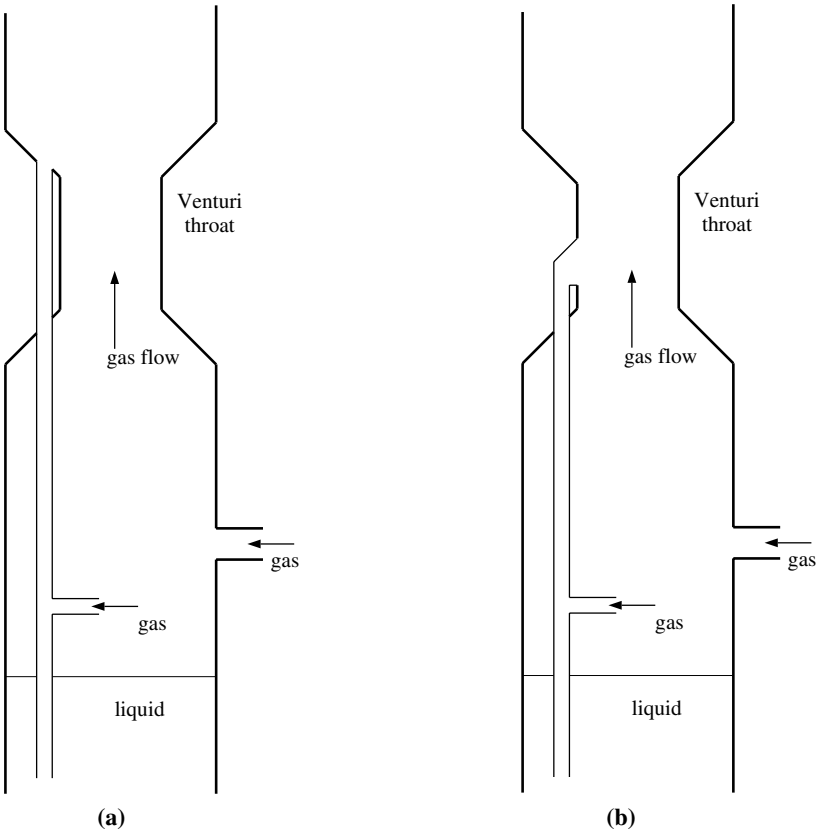

Fig. 16. (a) A modified geometry which, unlike that of Fig. 2, leaves the Venturi throat clear. (b) The configuration used in the experiments reported here.

flow. Much is known about atomization (Lefebvre, 1989); however, more complicated nozzles are likely to reduce the pressure available for lifting liquid from the bottom of the well.

The Venturi vented to the atmosphere. The absolute pressure p_G in the Venturi throat was typically 1 bar, and the differential pressure $P = p_B - p_G$ between the inlet and throat could be as much as 1 bar. The neglect of gas compressibility is therefore a poor approximation. However, in the analysis of Section 3 the gas density enters through $b = a_2(\rho_L/\rho_G)^{1/2}$, and so results vary only slowly with ρ_G. In the experiments the gas was air, at temperature approximately 15 °C. For modelling, the density of the air was taken to be $\rho_G = c_1 p/T$ (Kaye and Laby, 1995), where $c_1 = 0.00348\,\mathrm{kg\,m^{-3}\,K\,Pa^{-1}}$, at absolute temperature $T = 288\,\mathrm{K}$ and at the upstream absolute pressure $p = P_B = P + p_G$, with $p_G = 1\,\mathrm{bar}$.

The liquid was water, with density $\rho_L = 1000\,\mathrm{kg\,m^{-3}}$ and viscosity $\mu_L = 10^{-3}\,\mathrm{Pa\,s}$. At the base of the apparatus was a water reservoir with two water level sensors with vertical separation 200 mm, corresponding to a $0.004\,\mathrm{m^3}$ change in the volume of water. The distance h_1 between the gas inlet hole and the surface of the water therefore varied between 330 and 530 mm. This variation made little difference to the pressure P available for lifting liquid, since hydrostatic pressures in the gas (which affect p_B) are negligible. However, changes in h_1 caused changes in the liquid flow rate u_1 and the experimental results reported below are averages over the period of each test. An average distance $h_1 = 430\,\mathrm{mm}$ was used for the predictions presented in Figs. 17–20. The air/water mixture was raised a distance $h_2 = 2770\,\mathrm{mm}$.

In the model, gas enters the main riser through a pipe AF; in the experiments this was replaced by a circular hole in the riser wall. Experiments were performed with no hole at F (i.e. $a_2 = 0$), and with holes of diameter $d_2 = 3\,\mathrm{mm}$ or $d_2 = 5\,\mathrm{mm}$, corresponding to $a_2 = d_2^2/d_1^2 = 0.11$ or $a_2 = 0.31$. Fig. 17 shows the measured rate Q_L at which liquid was raised, as a function of the *measured* pressure difference P generated by the Venturi. The incompressible result (17) would have to be modified to include the effect of compressibility if used to predict P. However, pressures at the bottom of a gas well tend to be much larger than those used in the laboratory tests reported here, and the effect of compressibility would be correspondingly smaller. At the highest flow rates used in the experiments, the gas velocity in the throat of the Venturi reached $320\,\mathrm{m\,s^{-1}}$, and flow was

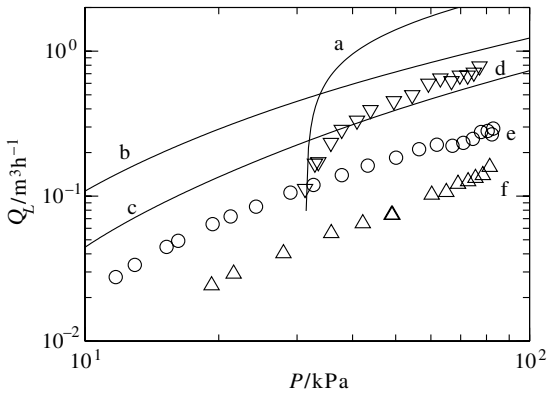

Fig. 17. Liquid volumetric flow rate Q_L as a function of the differential pressure P generated by the Venturi. Model predictions: (a) no hole for gas entry, (b) gas entry diameter $d_2 = 3\,\mathrm{mm}$, and (c) $d_2 = 5\,\mathrm{mm}$. Experimental values: (d) $\triangledown$ no hole, (e) $\bigcirc$ $d_2 = 3\,\mathrm{mm}$, and (f) $\triangle$ $d_2 = 5\,\mathrm{mm}$.

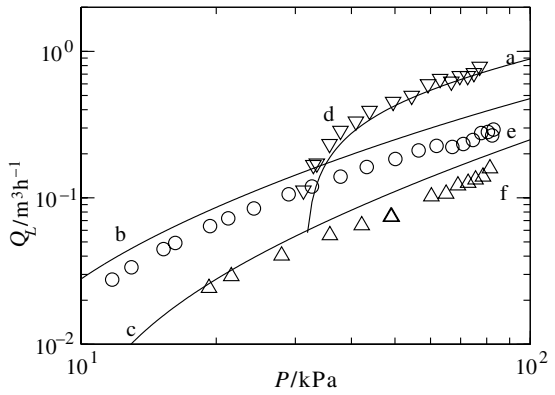

Fig. 18. As for Fig. 17, but with model predictions including a correction (92) for turbulent pressure losses, based upon a volume-averaged viscosity (96). Model predictions: (a) no hole for gas entry, (b) gas entry diameter $d_2 = 3\,\text{mm}$, and (c) $d_2 = 5\,\text{mm}$. Experimental values: (d) $\triangledown$ no hole, (e) $\bigcirc$ $d_2 = 3\,\text{mm}$, and (f) $\triangle$ $d_2 = 5\,\text{mm}$.

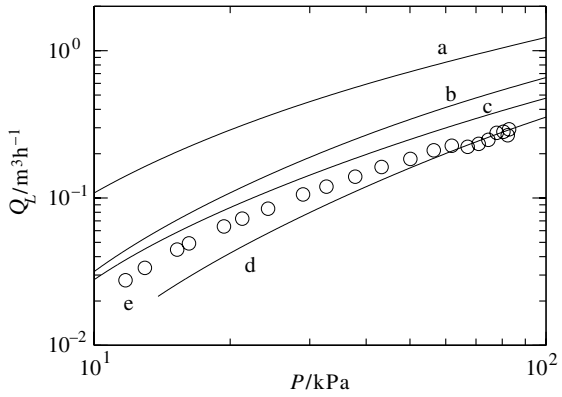

Fig. 19. Liquid volumetric flow rate Q_L as a function of the differential pressure P generated by the Venturi, with a hole of diameter $d_2 = 3\,\text{mm}$ for gas entry. (a) Model predictions without any correction for viscous losses. (b–d) Predictions including a correction (92) for turbulent pressure losses, taking the viscosity μ to be: (b) gas viscosity μ_G, (c) volume-averaged viscosity (96), and (d) liquid viscosity μ_L. (e) $\bigcirc$ experimental values $d_2 = 3\,\text{mm}$.

probably choked. This did not appear to have any effect on the entrainment of the gas/liquid mixture from the main riser.

We see from the experimental results of Fig. 17 that there is a minimum pressure $P = \rho_L g(h_1 + h_2) = 31\,\text{kPa}$ below which no liquid can be raised unless $a_2 > 0$. Also shown on Fig. 17 (curves a–c) are the predictions of the model. Although the general trends are correct, the predicted flow rates are in all cases higher than those observed experimentally. One reason for this is the neglect of pressure losses at entrances and corners; another reason is the neglect of viscous pressure losses within the device, which we now consider.

Single phase flow of fluid with viscosity μ and density ρ within the riser of diameter d_1 can be described in terms of the Reynolds number

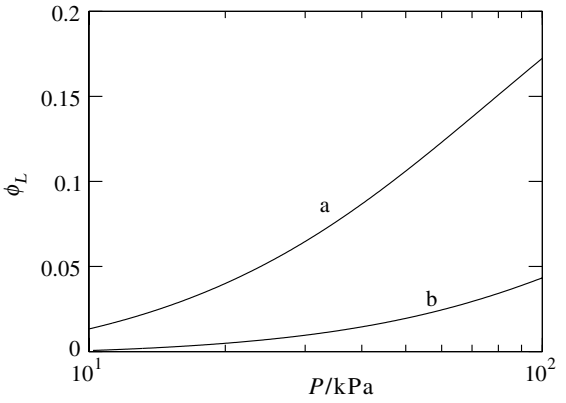

Fig. 20. The liquid volume fraction ϕ_L predicted when turbulent pressure losses are based on the volume-averaged viscosity (96). (a) Gas entry diameter $d_2 = 3$ mm, corresponding to curve (b) of Fig. 18; (b) $d_2 = 5$ mm, corresponding to curve (c) of Fig. 18.

$$Re = \rho U d_1/\mu, \tag{91}$$

where U is the mean fluid velocity. A simple correlation for turbulent frictional pressure drop Δp_f in a pipe of length h is (Millar, 1983)

$$\Delta p_f = 2\rho_L U^2 f h/d_1, \tag{92}$$

where the friction factor

$$f = 0.079\, Re^{-1/4} \tag{93}$$

so that the pressure drop is

$$\Delta p_f = 0.158 \frac{h U^{7/4} \rho^{3/4} \mu^{1/4}}{d_1^{5/4}}. \tag{94}$$

When $a_2 = 0$ there was no gas within the riser. We set $\mu = \mu_L$, $\rho = \rho_L$, and find that the flow rate $Q_L = 0.8\,\mathrm{m^3\,h^{-1}}$ corresponds to a velocity $u_3 = 3.5\,\mathrm{m\,s^{-1}}$ at Reynolds number $Re = 3 \times 10^3$. We conclude that flow was turbulent, so that viscous pressure losses can be estimated by (92). Once the flow rate had been predicted by the model of Section 3, the additional pressure required to overcome viscous losses was added to the inviscid pressure drop, with the pipe length $h = h_1 + h_2$ taken to be 3.2 m. The turbulent correlation (94) was used in all cases: when at low Reynolds number the flow is laminar, pressure losses are small and errors in their estimation are of little importance. The predictions of this modified analysis, shown in Fig. 18 (curve a), are in good agreement with experiment.

When $a_2 > 0$ gas enters the main riser. Much less is known about turbulent pressure drop in gas–liquid flow than in single-phase flow. A simple modified form of the correlation (94) was therefore used. The analysis of Section 3 predicted the volume fraction ϕ_L of liquid in the gas–liquid mixture, and the liquid density ρ_L in (94) was replaced by the volume-averaged mixture density

$$\rho = \phi_L \rho_L + (1 - \phi_L)\rho_G. \tag{95}$$

The fluid viscosity μ was similarly taken to be the volume average

$$\mu = \phi_L \mu_L + (1 - \phi_L)\mu_G \tag{96}$$

with the viscosity of air $\mu_G = 18\,\mu\text{Pa s}$ (Kaye and Laby, 1995). This volume average has no physical justification, but the choice is relatively unimportant since the correlation (94) does not depend strongly on viscosity μ.

The height h in the expression (94) for turbulent pressure loss was taken to be the length of pipe above the point of gas entry (2.77 m); losses in the lower 0.43 m liquid-filled portion of pipe (DE in Fig. 2), where velocities are smaller, were neglected. We see from Fig. 18 that the predictions (curves b and c) are in agreement with the experiment. Given the crudeness of the model for turbulent pressure losses, such good agreement seems somewhat fortuitous. Gas is likely to be the continuous phase in the mixture, so that the volume-averaged viscosity (96) and the corresponding friction pressure loss (94) are probably too high. However, this compensates for the neglect of pressure losses at the point of gas entry into the rising liquid and for losses at the bend just before the gas–liquid mixture enters the Venturi throat.

We see from (94) that the turbulent viscous losses do not depend strongly on viscosity. Fig. 19 (curve a) shows the volumetric flow rate Q_L predicted in the absence of viscosity, together with the experimental results (labelled e). Also shown are the flow rates predicted when the turbulent pressure loss (94) is included, with the mixture viscosity taken to be either (b) the gas viscosity μ_G, (c) the mixture viscosity (96) or (d) the liquid viscosity μ_L. The volume fraction of liquid is always small. Fig. 20 shows the predicted ϕ_L as a function of the differential pressure P when the average viscosity (96) is used.

Once gas enters the main riser the velocity u_3 depends not only on the liquid flow rate Q_L but also on the liquid volume fraction ϕ_L. When $P = 80\,\text{kPa}$ the model predicts $Q_L = 0.39\,\text{m}^3\,\text{h}^{-1}$ and $\phi_L = 0.15$, so that $u_3 = 11\,\text{m s}^{-1}$; churn flow was observed. The density ρ_3 of the mixture is given by (5), and the mean bulk modulus is

$$K_3 = \left(\frac{\phi_L}{K_L} + \frac{1 - \phi_L}{K_G}\right)^{-1}, \tag{97}$$

where the isothermal bulk modulus of the gas is $K_G = p$ and the bulk modulus of the liquid is $K_L \gg K_G$. This leads to an estimate for the isothermal sound velocity,

$$c \approx \left(\frac{p}{\rho_L \phi_L (1 - \phi_L)}\right)^{1/2}, \tag{98}$$

which gives $c \approx 28\,\text{m s}^{-1}$ at $p = 1\,\text{bar}$ and $\phi_L = 0.15$. We conclude that flow in the main riser was unlikely to be choked in the experiments. However, this possibility ought to be checked when a practical design is attempted.

8. Concluding remarks

The results presented in Section 3 assumed $\rho_G \ll \rho_L$ and $a_2 \ll 1$. These assumptions were made in order to reduce the number of independent governing parameters from four, namely G, ρ_L/ρ_G,

h_1/h_2 and a_2 to three: G, h_1/h_2 and $b = a_2(\rho_L/\rho_G)^{1/2}$. If ρ_G/ρ_L is known (but not necessarily small), it is straightforward to solve (29) numerically and thereby investigate the effect of varying a_2; there is no need to work solely with the combination $b = a_2(\rho_L/\rho_G)^{1/2}$.

We have not attempted to estimate the rate at which liquid will return to the bottom of the well via thin films on either the wall of the wellbore or the wall of the riser FG. In a long wellbore the probability of a liquid droplet hitting, and being captured by such a wall film is large. There also remain technical design issues related to the best way to inject gas into the main riser, which we have not addressed here.

A flow of gas is required to generate the differential pressure P that drives the device, which must therefore be installed and in operation before the liquid level at the bottom of the well rises so far that gas flow is blocked.

References

Batchelor, G.K., 1967. An Introduction to Fluid Mechanics. Cambridge University Press.

Kay, J.M., Nedderman, R.M., 1974. An Introduction to Fluid Mechanics and Heat Transfer, third ed. Cambridge University Press.

Kaye, G.W.C., Laby, T.H., 1995. Tables of Physical and Chemical Constants, 16th ed. Longman.

Lefebvre, A.H., 1989. Atomization and Sprays. Hemisphere, New York.

Millar, R.W., 1983. Flow Measurement Engineering Handbook. McGraw-Hill, New York.

Miller, D.S., 1978. Internal Flow Systems. BHRA Fluid Engineering, Cranfield, UK.

Sherwood, J.D., Atkinson, I., Nicholson, B., 2003. Method and apparatus for lifting liquids from gas wells. UK Patent application 0312652.1.